Experimental Hematology

Experimental Hematology 2015;43:1047–1061

Zebrafish embryonic stromal trunk (ZEST) cells support hematopoietic stem and progenitor cell (HSPC) proliferation, survival, and differentiation

Clyde Campbell[a], Tammy Su[a], Ryan P. Lau[a], Arpit Shah[b], Payton C. Laurie[b], Brenda Avalos[b], Julian Aggio[b], Elena Harris[b], David Traver[a], and David L. Stachura[b]

[a]*Department of Cellular and Molecular Medicine, University of California at San Diego School of Medicine, La Jolla, California, USA;* [b]*Department of Biological Sciences, California State University, Chico, California, USA*

(Received 1 June 2015; revised 11 August 2015; accepted 3 September 2015)

Forward genetic screens in zebrafish have been used to identify genes essential for the generation of primitive blood and the emergence of hematopoietic stem cells (HSCs), but have not elucidated the genes essential for hematopoietic stem and progenitor cell (HSPC) proliferation and differentiation because of the lack of methodologies to functionally assess these processes. We previously described techniques used to test the developmental potential of HSPCs by culturing them on zebrafish kidney stromal (ZKS) cells, derived from the main site of hematopoiesis in the adult teleost. Here we describe an additional primary stromal cell line we refer to as zebrafish embryonic stromal trunk (ZEST) cells, derived from tissue surrounding the embryonic dorsal aorta, the site of HSC emergence in developing fish. ZEST cells encouraged HSPC differentiation toward the myeloid, lymphoid, and erythroid pathways when assessed by morphologic and quantitative reverse transcription polymerase chain reaction analyses. Additionally, ZEST cells significantly expanded the number of cultured HSPCs in vitro, indicating that these stromal cells are supportive of both HSPC proliferation and multilineage differentiation. Examination of ZEST cells indicates that they express numerous cytokines and Notch ligands and possess endothelial characteristics. Further characterization of ZEST cells should prove to be invaluable in understanding the complex signaling cascades instigated by the embryonic hematopoietic niche required to expand and differentiate HSPCs. Elucidating these processes and identifying possibilities for the modulation of these molecular pathways should allow the in vitro expansion of HSPCs for a multitude of therapeutic uses.

Hematopoiesis, the production of blood, is an essential cellular process that occurs constantly over an organism's life span and is a paradigm for stem cell biology [1]. This process starts with the hematopoietic stem cell (HSC), a tissue-specific stem cell that has the ability to both self-renew and differentiate into more developmentally restricted progenitor cells that subsequently mature into the full repertoire of blood and immune cells. Importantly, this process is tightly regulated; perturbations in the proliferation and differentiation of hematopoietic stem and progenitor cells (HSPCs) can lead to a host of hematopoietic disorders, including anemia, thrombocytopenia, leukopenia, and leukemia.

Zebrafish provide an excellent vertebrate model system to study hematopoiesis [2–4]. Their external development, high fecundity, and optical transparency have made them instrumental in the visualization of de novo HSC production [5,6] and leukocyte behavior [7–10]. Zebrafish possess the full repertoire of mammalian blood cells including an innate [11–13] and adaptive immune system [14,15], and the genetic control of hematopoiesis is well conserved among fish and mammals. Importantly, zebrafish are useful in permitting large-scale forward genetic mutagenesis [16–18] and drug screens [19–23]. Their utility as a screening platform has resulted in identifying genes required for primitive hematopoiesis [18,24] and drugs now in clinical trials to treat hematologic disorders [25].

Because the zebrafish is a relatively new model system, functional means of identifying bona fide HSPCs have been lacking. Clonal lines of zebrafish have only recently been developed [26–28], making transplantation of HSPCs into

Offprint requests to: David L. Stachura, Department of Biological Sciences, California State University, 400 West 1st Street, Chico, CA 95929-0515; E-mail: dstachura@csuchico.edu; davidstachura@gmail.com

0301-472X/Copyright © 2015 ISEH - International Society for Experimental Hematology. Published by Elsevier Inc.
http://dx.doi.org/10.1016/j.exphem.2015.09.001

immune-matched hosts problematic. Although advances have been made in HSPC transplantation [29], these experiments are still technically difficult. To approach this problem in another way, we developed the first in vitro assays to test HSPC function. Our original approach was to create zebrafish kidney stroma (ZKS) cells [30], a primary cell line derived from the main site of hematopoiesis in the adult zebrafish. The development of this line allowed us to identify cytokines produced by ZKS cells, permitting the development of clonal methylcellulose assays to test HSPC development [31]. As mammalian cytokines exhibit little cross-reactivity with paralogous zebrafish receptors [32], the identification and validation of zebrafish cytokines have proven invaluable for understanding signaling molecules involved in teleost hematopoiesis.

To identify more cytokines responsible for zebrafish HSPC proliferation and differentiation, we isolated tissue near the embryonic dorsal aorta, the first site of definitive hematopoiesis and HSC formation in the zebrafish, culturing these cells in vitro. We have termed these primary cells *zebrafish embryonic stromal trunk* (ZEST) cells. Although ZEST cells do not express hematopoietic markers, they do encourage the proliferation and differentiation of HSPCs in culture. We also illustrate that ZEST cells can easily be used for quantification of multilineage HSPCs. Like their adult hematopoietic stromal counterparts, ZEST cells produce hematopoietic-supportive cytokines; further characterization of their transcriptome should elucidate molecules important for the generation, expansion, and differentiation of vertebrate HSCs and HSPCs.

Methods

Zebrafish stocks and embryos

Zebrafish were mated, staged, raised, and maintained in accordance with University of California, San Diego, and California State University, Chico, IACUC guidelines. AB* wild-type (wt) fish and the transgenic *tg(–6.0itga2b:eGFP)* [33] (referred to throughout as *cd41:GFP)* and *tg(–3.5ubi:EGFP)* [34] (referred to throughout as *ubi:GFP)* were used.

Generation of ZEST cells

Zebrafish embryonal stromal trunk cells were isolated by surgically removing the dorsal aorta and surrounding tissue from the trunk of 48-hour postfertilization (hpf) AB* wt fish. At 48 hpf, approximately 200 embryos were rinsed three times in sterile embryo medium in 10-cm^2 plates. By use of an Olympus SZ51 dissecting microscope, the tissue posterior to the yolk tube extension was removed and discarded. Then, the tissue anterior to the yolk tube extension (including the large yolk ball) was removed with a sterile scalpel and discarded (Fig. 1A, *hatched area* denotes the region that was isolated). The remaining trunk of the embryo was finely minced with a surgical scalpel and grown in zebrafish tissue culture medium [30] in a 12.5-cm^2 tissue culture flask. The mincing of the tissue destroyed most of the ventral yolk tube extension, but any that remained in the culture medium did not attach to the surface of the flasks. The cells that attached to the surface of the flask were grown at 32°C in 5% CO_2 until cells achieved ≥80% confluence. Cells were trypsinized for 5 min and expanded onto 75-cm^2 tissue culture flasks.

Morphologic characterization of ZEST cells

Zebrafish embryonic stromal trunk cells were grown on glass coverslips in culture medium in 24-well tissue culture plates. When cells reached 100% confluence, they were fixed and stained with May–Grünwald–Giemsa and visualized by microscopy [35].

Reverse transcription polymerase chain reaction analysis of ZEST cells

RNA was isolated from ZEST cells using a QIAGEN RNeasy kit, and cDNA was generated using the BioRad iScript cDNA synthesis kit. Primers, product sizes, and annealing temperatures used for the reverse transcription polymerase chain reaction (RT-PCR) characterization of ZEST cells are listed in Table 1.

Isolation and enumeration of whole kidney marrow cells

Whole kidney marrow (WKM) cells were isolated as described previously [35] and enumerated by trypan blue exclusion and counting with a hemocytometer. WKM cells were added on top of ZEST cells when the stroma was 80% confluent; ZEST cells divide slowly and do not need to be mitotically arrested with mitomycin C or irradiation. To enumerate WKM cells after culture on ZEST cells, the stroma was gently rinsed to remove the WKM from the cell monolayers. Cells were concentrated by centrifugation at 300*g*, cytospun onto slides, stained with May–Grünwald–Giemsa, and visualized by microscopy.

Quantitative RT-PCR analysis of cultured hematopoietic cells

RNA was isolated from cultured ZEST cells using a QIAGEN RNeasy kit, and cDNA was generated using a BioRad iScript cDNA synthesis kit. Quantitative RT-PCR (qRT-PCR)was performed on an Eppendorf Mastercycler with BioRad SsoAdvanced Universal SYBR Green Supermix. Primers have been previously described [38,39]. Fold expression was determined by the $\Delta\Delta Ct$ method, using ef1α as a reference gene and kidney as a reference tissue.

Fluorescence-activated cell sorting

Whole kidney marrow from *ubi:GFP* fish was isolated and resuspended in phosphate-buffered saline with 0.9% fetal bovine serum. Lymphoid and precursor fractions were sorted and analyzed on a FACSAriaII (BD Biosciences) by using their unique forward and side scatter characteristics [40]. Sytox red (Life Technologies) was used as a cell viability stain.

Proliferation of HSPCs on ZEST cells by flow cytometry

Lymphoid and precursor fractions from WKM were isolated and stained with the membrane dye PKH-26 (Sigma) and plated onto monolayers of ZEST cells. PKH-26 fluorescence was analyzed before the cells were plated and after 5 days in culture on an LSRII flow cytometer (BD Biosciences). Proliferation calculations were performed with FloJo software Version 9 (Treestar), specifically using the Proliferation Platform, which was used to determine the percentage of WKM cells that divided, as well as the culture's division index. The division index is defined as the average number of cell divisions a WKM cell underwent over the course of the experiment.

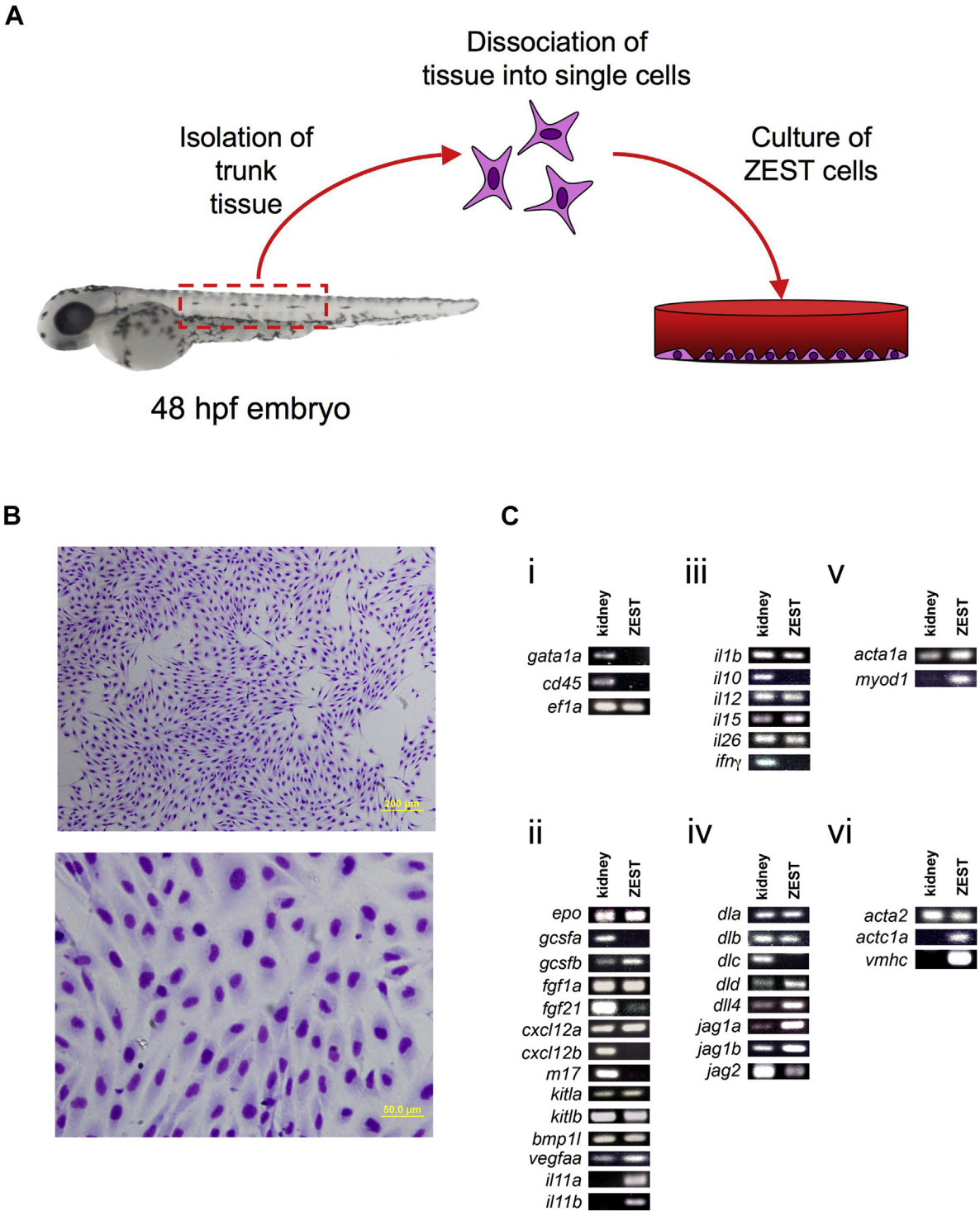

Figure 1. ZEST cells are a primary stromal cell line derived from the zebrafish embryonic trunk tissue that expresses hematopoietic-supportive transcripts. **(A)** Schematic illustration of isolation and culture of ZEST cells from 48-hpf zebrafish embryos. **(B)** Morphologic characterization of ZEST cells with May–Grünwald–Giemsa staining indicates stromal morphology. Top image photographed at 400 × (bar = 200 μm); bottom image photographed at 1,000 × (bar = 50 μm). **(C)** Gene expression analysis of ZEST cells by RT-PCR for various transcripts. ZEST cells do not express the pan-leukocytic transcript *cd45* or the erythroid-specific transcription factor *gata1* (i). ZEST cells express certain transcripts involved in the proliferation and differentiation of progenitor cells (ii); hematopoietic lineage-specific signaling, maintenance, and differentiation (iii); Notch signaling and lymphoid development (iv); muscle differentiation and development (v); and cardiac development (vi). Gene names are listed at left and whole kidney was used as a positive control. Distilled H_20 controls were also universally negative, although not shown. RT-PCR primer sequences are listed in Table 1.

Table 1. Primer sets used for RT-PCR characterization of ZEST cells. Gene names are listed at far left, followed by the gene's description

Gene	Definition	Forward primer (5′–3′)	Reverse primer (5′–3′)	Annealing Temperature (°C)	Product Size (bp)
acta1a	*Danio rerio* actin, α1a, skeletal muscle	GAAAAGAGCTACGAGCTTCC	GTAAGTGGTCTCGTGAATGC	50°	129
acta2	*Danio rerio* actin, α2, smooth muscle	TGGATCTGGACTGTGTAAGG	ACTATCTTTCTGCCCCATTC	50°	121
actc1a	*Danio rerio* actin, α, cardiac muscle 1a	TGCTGTCTTTCCCTCTATTG	GAGTGAGGATACCCCTCTTG	50°	116
bmp1l [30]	*Danio rerio* bone morphogenic protein 1, like	GGATGGATATTGGAGGAAAG	CTTTGTTCGGTCTGTAATCG	50°	230
gcsfa (csf3) [36]	*Danio rerio* colony stimulating factor 3a, granulocyte colony stimulating factor	AACTACATCTGAACCTCCTG	GACTGCTCTTCTGATGTCTG	55°	165
cxcl12a	*Danio rerio* chemokine (C–X–C motif) 12a, stromal cell-derived factor 1a	CGCCATTCATGCACCGATTTC	GGTGGGCTGTCAGATTTCCTTGTC	50°	297
cxcl12 b	*Danio rerio* chemokine (C–X–C motif) 12b, stromal cell-derived factor 1b	CGCCTTCTGGAGCCCAGAGA	AGAGATTCTCCGCTGTCCTCC	50°	291
dla [30]	*Danio rerio* δA	ACGACGATTTGAGTATGACG	GGGATTGGCACTTTATATCC	50°	186
dlb [30]	*Danio rerio* δB	TTCCGTGTTTAATGATTTGG	CACTCCACAGAAACTCTTGC	50°	158
dlc [30]	*Danio rerio* δC	TGGTGGACTACAATCTGAGC	ACCTCAGTAGCAAACACACG	50°	169
dld	*Danio rerio* δD	AACCCAGACCGTCTGATCAGT	CCGGGTTTGTCGCAAAAGCCA	50°	308
*dll4*_ENREF_30 [30]	*Danio rerio* δ-like 4	CTCTTTCAGCACACCAATTC	TGAACATCCTGAGACCATTC	50°	189
ef1a (eef1a1l1) [37]	*Danio rerio* eukaryotic translation elongation factor 1 alpha 1, like 1	GAGAAGTTCGAGAAGGAAGC	CGTAGTATTTGCTGGTCTCG	55°	123
epo [30]	*Danio rerio* erythropoietin	ACTTGTAAGGACGATTGCAG	TATCTGTAATGAGCCGATGG	55°	156
fgf1 [30]	*Danio rerio* fibroblast growth factor 1	ATACTGCGCATAAAAGCAAC	AGTGGTTTTCCTCCATCTTC	50°	154
fgf21 [30]	*Danio rerio* fibroblast growth factor 21	CGGTGGTGTATGTATGTTCC	GTAGCTGCACTCTGGATGAC	50°	203
gata1a [37]	*Danio rerio* GATA binding protein 1a	TGAATGTGTGAATTGTGGTG	ATTGCGTCTCCATAGTGTTG	55°	650
gcsfb (csf3b) [36]	*Danio rerio* colony-stimulating factor 3b, granulocyte colony-stimulating factor b	GGAGCTCTGCGCACCCAACA	GGCAGGGCTCCAGCAGCTTC	55°	184
ifnγ	*Danio rerio* interferon, γ 1-2	TACATAATGCACACCCCATC	TCCTTTGTAGCTTCATCCAC	55°	158
il-1b	*Danio rerio* interleukin-1, β	TCCACATCTCGTACTCAAGG	CAGCTCGAAGTTAATGATGC	50°	227
il-10 [30]	*Danio rerio* interleukin-10	ATGAATCCAACGATGACTTG	TCTTGCATTTCACCATATCC	50°	222
il-11a [30]	*Danio rerio* interleukin-11a	GACAAGCTGAGCAATCAGAC	GGAGCTGAGAAAGAGTAGGC	50°	172
il-11b [30]	*Danio rerio* interleukin-11b	TTGAACATTCGCTATCATCC	GAGTAATCGTTCCCCAATTC	50°	166
il-12a [30]	*Danio rerio* interleukin-12a	GTGAGTCTGCTGAAGGAGTG	AGTGACATCATTTCCTGTGC	50°	167
il-15 [30]	*Danio rerio* interleukin-15, like	CCAAGTCCACAATTACATGC	TCTTTGTAGAGCTCGCAGAC	55°	166
il-26 [30]	*Danio rerio* interleukin-26	TGAAAAGATGTGGGATGAAC	ACTGATCCACAGCAAAACAC	55°	214
jag1a [30]	*Danio rerio* jagged 1a	TGATTGGTGGATACTTCTGC	AATCCATTGAGTGTGTCCTG	55°	238
jag1b [30]	*Danio rerio* jagged 1b	CTGTGAGCCATCTTCTTCAG	AGCAAAGGAACCAGGTAGTC	55°	213
jag2 [30]	*Danio rerio* jagged 2	AATGACTGTGTGAGCAATCC	GTCATTGACCAGATCCACAC	50°	174
kitlga [30]	*Danio rerio* kit ligand a	GGATTCAATGCTTGACTTTG	TGTACTATGTTGCGCTGATG	50°	205
kitlgb	*Danio rerio* kit ligand b	GGCAACCAGTCCACCAATAAG	CACTTTTCCCTTCTGTAGTGGC	50°	135
m17	*Danio rerio* il-6 subfamily cytokine M17	CTTGATTGCCGTTCAGTTAG	TGACCGGAGATTGTAGACAC	50°	210
myod1	*Danio rerio* myogenic differentiation 1	ATGGCATGATGGATTTTATG	TTTATTATTCCGTGCGTCAG	50°	107
cd45 (ptprc) [37]	*Danio rerio* protein tyrosine phosphatase, receptor type, C	AGTTCCTGAAATGGAAAAGC	GCACAGAAAAGTCCAGTACG	55°	140
vegfaa	*Danio rerio* vascular endothelial growth factor Aa	GAAACGTCACTATGGAGGTG	TTCTTTGCTTTGACTTCTGC	50°	121
vmhc	*Danio rerio* ventricular myosin heavy chain	TTATTGACTTTGGCATGGAC	AAAATGAGACTCTGGCTTCC	50° 50°	203

Differentiation analysis of HSPCs on ZEST

Single *cd41:GFP*$^{+}$ cells from the lymphoid fraction were plated into individual wells of 96-well plates on top of ZEST monolayers. Iron supplement (1:1,000, Sigma) and carp serum (1:1,000) was added to each well to encourage erythroid development [30]. After 5 days of *cd41:GFP*$^{+}$ cell growth and differentiation, RNA was collected from the wells and processed for qRT-PCR. Quantitative RT-PCR was performed with primers specific for erythroid, myeloid, and lymphoid differentiation. As a control, plates with ZEST cells only were also processed and analyzed for the same transcripts. Individual cell sorting into plates was verified by microscopic analysis of fluorescent cells.

Sequence alignment and read counts

All sequenced libraries were processed using the following procedures. First, copy-duplicates were removed from sequenced reads. Two sequenced reads are considered to be copy-duplicates, the product of PCR, if they are exact copies of each other. Only one copy of exact copy-duplicates was kept. Quality control was carried out using FastQC tool (http://www.bioinformatics.babraham.ac.uk/projects/fastqc/). Because base sequence content (count of A, C, G, T along the reads' lengths) in the first 10 bp of the reads exhibited an abnormal distribution, the first 10 bases were trimmed. Another measurement, namely, *k*-mer content of FastQC, revealed high *k*-mer enrichment at the end of reads. A *k*-mer is a short *k*-base-long substring of a read. Various adapter trimming tools were used to reduce adapter contamination, and, hence, *k*-mer enrichment; however, none of the tools used significantly affected the results of *k*-mer enrichment. Therefore, to reduce *k*-mer enrichment, we used our own method to trim unaligned ends of the reads (potential adapter contamination). First, the sequenced reads were aligned, using the *bowtie-2* tool [41], to cDNA sequences of zebrafish (zv9, Ensembl), using *local* mode of alignment and loose parameters that allowed mapping with low alignment score, with the following options: –score-min L,–2,0.3, –L 18, –ma 3, –mp 1,1, –np 1, –rdg 50,50, –rfg 50,50, –ignore-quals, –k 1. Then our own script processed the results of the alignments and extracted only high-quality aligned consecutive stretches of the reads, requiring the minimum length of this stretch to be at least 32 bp. In other words, loosely mapped ends of the sequenced reads were trimmed. Next, trimmed reads were mapped to cDNA sequences using bowtie-2 with default parameters and option–k 23 (this option finds at most 23 alignments for each read). Because there are at most 22 different transcripts for each gene in zebrafish, this option ensured the finding of alignments to different genes. On the basis of the mapping results, only uniquely mapped reads were kept for further analysis. A read was considered *unique* if it was mapped to the transcripts of the same gene only; in other words, if a read was mapped to transcripts of two different genes with the same best alignment score, then the read was considered to be ambiguous and was discarded from further analysis. Our own script was used together with the Ensembl GTF file with the gene information of zebrafish to count the total number of unique reads mapped to each gene. These read counts were used to identify differentially expressed genes in each sample compared with the negative control, ZF4 cells.

Normalization and differential expression

To identify differentially expressed genes in ZEST/ZKS samples compared with the ZF4 cells, the Microsoft online tool FDR Calculator based on Fisher's exact test was used: http://research.microsoft.com/en-us/um/redmond/projects/mscompbio/falsediscoveryrate/default.aspx. The tool calculated the p and q values for each gene from the read counts. A gene was considered to be differentially expressed in a sample ZEST/ZKS compared with ZF4 if its p value was ≤ 0.05, and its q value was ≤ 0.1, and the maximum read count in two samples was at least 10. To identify overexpressed genes in a sample ZEST/ZKS compared with ZF4, we used RPKM (reads perkilo base per million mapped reads), calculated as the read count multiplied by 10^9 and divided by the gene's length and total read count per sample. The gene's length was calculated as the sum of lengths of all its exons. If the RPKM value for a differentially expressed gene in a sample ZEST/ZKS was greater than the RPKM value for the same gene in sample ZF4, then the gene was considered overexpressed.

To compare overexpressed genes in ZEST and ZKS samples, only overexpressed genes with a twofold change in a ZEST/ZKS sample compared with ZF4 were considered. The Venn diagrams were built using overexpressed genes in ZEST/ZKS whose RPKM value in a ZEST/ZKS sample was at least twice its RPKM value in the ZF4 sample.

To build the heat-map clustergram, we considered the top 100 overexpressed genes with a twofold change in a ZEST/ZKS sample compared with the ZF4 sample. Of these, the genes with the highest average RPKM values were used to build the heat-map clustergram.

Results

ZEST cells are derived from embryonic trunk stroma

Because the site of HSC emergence in zebrafish is endothelium located in the floor of the dorsal aorta [5,6], we hypothesized that stromal cells isolated from this embryonic area would support hematopoiesis. To create ZEST cells, we dissociated the trunk tissue of 48-hpf wt embryos by removing tissue anterior and posterior to the yolk tube extension (Fig. 1A). The tissue dorsal to the yolk tube extension was then finely minced with a scalpel and grown in zebrafish tissue culture medium [30] in tissue culture flasks until cells were confluent. On confluence, cells were trypsinized and passaged for further culture. Although cells were not transformed in any way, they have continued in culture for more than 90 passages with no signs of senescence (data not shown).

Cultured ZEST cells displayed a fibroblastic morphology when grown on glass coverslips and stained with May–Grünwald–Giemsa (Fig. 1B). To confirm that these ZEST cells were of stromal origin and did not contain hematopoietic cell lineages, RT-PCR was performed for both the pan-leukocytic marker *cd45* and the red blood cell-specific *gata1* (Fig. 1Ci). Neither of these transcripts were present, confirming that ZEST cultures were not hematopoietic or contaminated with mature hematopoietic cells.

To further characterize these cells at the transcriptional level, RT-PCR was performed to analyze the expression

of genes known to play essential roles in hematopoietic maintenance, development, and proliferation. Transcriptional analysis revealed that ZEST cells expressed many hematopoietic progenitor-supportive factors including *kitla*, *kitlb*, *bmp1l*, *fgf1a, fgf21*, *il-11a*, and *il-11b*, as well as cytokines and growth factors involved in lineage-specific signaling, maintenance, and differentiation, such as *epo* [42], *gcsfa* [43], and *gcsfb* [36] (Fig. 1Cii), and inflammatory signaling (Fig. 1Ciii). Additionally, ZEST cells expressed Notch ligands involved in niche signaling, lymphocyte development, and maturation (Fig. 1Civ). Finally, ZEST cells expressed transcripts indicative of skeletal (Fig. 1Cv) and smooth (Fig. 1Cvi) muscle. Together, these data indicate that ZEST cells are stromal and produce a multitude of ligands important for the survival and proliferation of hematopoietic cells.

ZEST cells support hematopoiesis and promote hematopoietic proliferation

The main site of adult hematopoiesis in teleosts is the kidney; all mature blood cell types can be isolated from WKM [40], as well as hematopoietic stem and progenitor cells (HSPCs) [31,36,40,44]. To determine if ZEST cells were capable of supporting hematopoiesis, WKM from adult wt fish was plated on an 80% confluent layer of ZEST cells. WKM cells plated on ZEST cells or without stromal support were quantified at days 3, 6, 9, and 14. Compared with cells cultured without supportive stroma, WKM cells proliferated in the presence of ZEST cells, increasing nearly five times over the course of 2 weeks (Fig. 2A). To confirm that these expanding cells were hematopoietic, we examined cytocentrifuge preparations at each time point, analyzing their cellular morphologies (Fig. 2B). Although mature red blood cells persisted for only 6 days in culture, myeloid, lymphoid, and precursor cells were observed at all time points, indicating that ZEST cells are capable of maintaining these hematopoietic cell lineages in culture. Importantly, the support of hematopoiesis required cell–cell interaction between WKM cells and ZEST stoma; conditioned medium from these stromal cells was incapable of expanding WKM (data not shown).

To investigate the ability of ZEST cells to encourage proliferation of HSPCs, we isolated purified lymphoid and precursor populations from fish by fluorescence-activated cell sorting (FACS). We used *ubi*:GFP [34] fish for these experiments because their blood is uniformly GFP$^+$, allowing us to ensure that the our results were from the plated hematopoietic cells, and not the ZEST cells themselves. The small, agranular lymphoid fraction contains B and T lymphocytes, as well as HSPCs [30,31,40,44]. The precursor fraction is slightly larger and more granular, and contains myeloid, lymphoid, and erythroid progenitors [30,31,40,44]. These FACS-isolated cell populations were cultured on 80% confluent ZEST monolayers and quantified at days 3, 6, 9, and 13

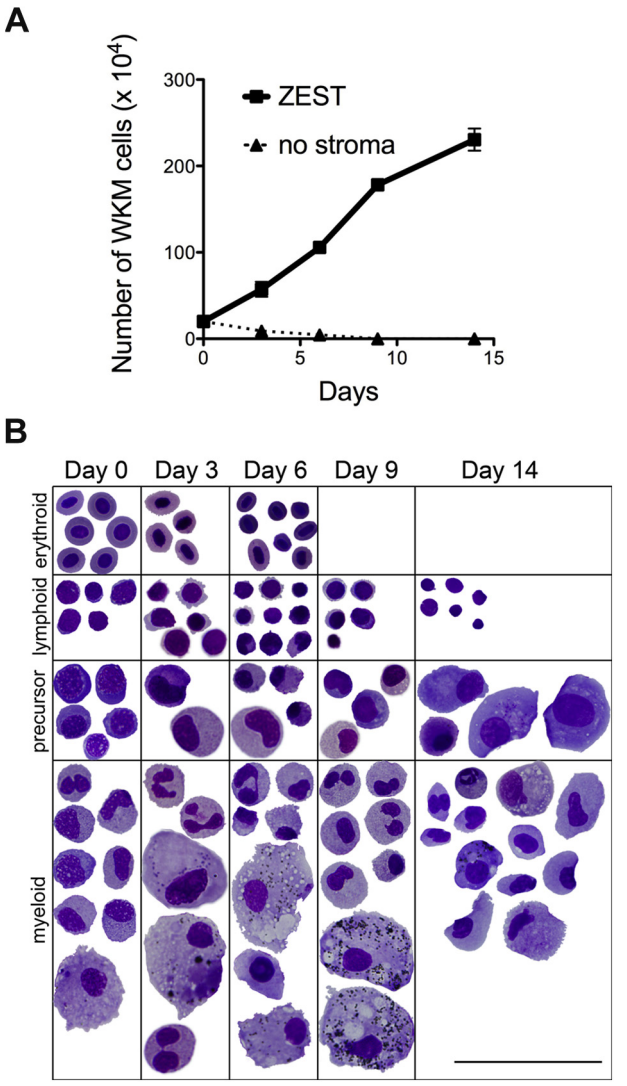

Figure 2. ZEST cells encourage WKM proliferation and support hematopoiesis. **(A)** WKM cells plated on ZEST monolayers (*squares, solid line*) or with no stroma (*triangles, dashed line*) were enumerated over 14 days. **(B)** WKM cells from **(A)** were cytospun and stained with May–Grünwald–Giemsa stain. Cell images were taken at 1,000 × (bar = 25 μm), and grouped into erythroid (top row), lymphoid (second row), precursor (third row), and myeloid (bottom row) morphologies.

(Fig. 3A). Expansion of cells from the lymphoid and precursor cell fractions was observed at all time points, indicating that ZEST cells facilitate HSPC proliferation. To further corroborate these data, purified *ubi*:GFP$^+$ lymphoid and precursor cell fractions were stained with the fluorescent red membrane dye PKH-26 and either plated on a monolayer of confluent ZEST cells or plated without supportive stroma. After 5 days, these cells were examined by flow cytometry for relative fluorescence intensity. Cells stained with PKH-26 maintain their red fluorescence until they divide, which decreases their fluorescence intensity by 50%. After 5 days in culture, more than 60% of cells from the precursor fraction and 10% of the cells from the

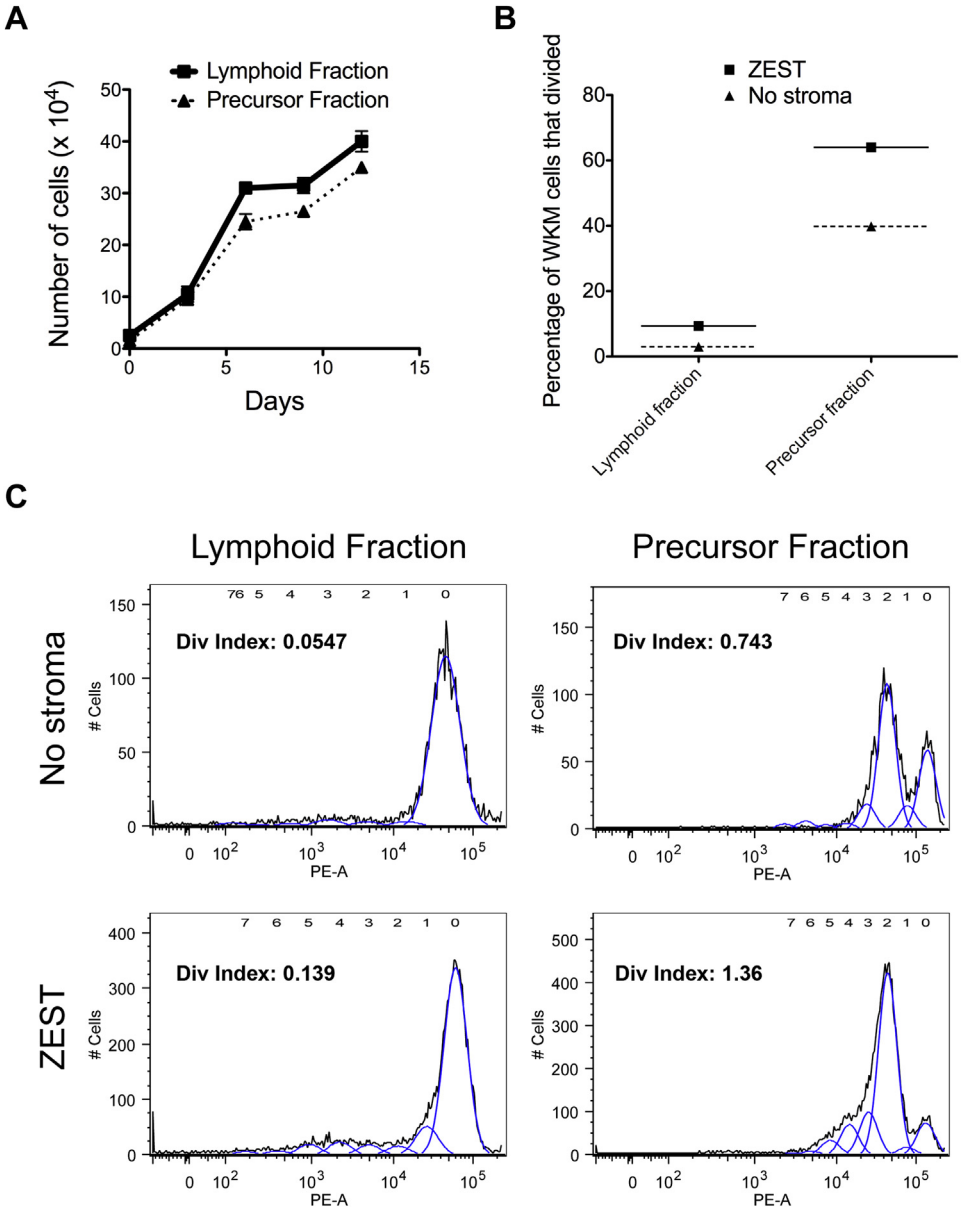

Figure 3. ZEST cells encourage proliferation of lymphoid and precursor cell fractions. **(A)** Enumeration of WKM cells generated from isolated lymphoid (*squares, solid line*) and precursor (*triangles, dashed line*) cell populations plated on ZEST cells over 14 days. **(B)** Cells stained with the cell membrane dye PKH-26 from isolated lymphoid (left) and precursor (right) cell fractions grown on ZEST cells (*squares, solid line*) or with no stromal support (*triangles, dashed lines*). After 5 days in culture, WKM cells derived from these cultures were analyzed by flow cytometry, and FloJo's Proliferation Platform was used to calculate the percentage of cells in the cultures that divided. **(C)** Cells stained with the cell membrane dye PKH-26 (PE-A, *x* axis) from isolated lymphoid (left) and precursor (right) cell fractions grown with no stromal support (top) or on ZEST cells (bottom). After 5 days in culture, cells were analyzed by flow cytometry to determine how many rounds of cell division occurred without (top) or with (bottom) ZEST support. Numbers (0–7) above the histograms (*blue lines*) represent the number of divisions that occurred over 5 days, with 0 corresponding to cells that did not undergo division. The *blue histogram lines* are calculated and drawn by the Proliferation Platform module within the FloJo software package. The numbers above each blue peak correspond to the number of divisions that each population underwent, and the height of the peak corresponds to the numbers of cells that divided. The program also calculates a division index of each culture, defined as the average number of cell divisions that a WKM cell underwent over 5 days. (Color version available online.)

lymphoid fraction exhibited at least 1 cell division event when cultured on a ZEST monolayer (Fig. 3B). Additionally, the lymphoid and precursor cells plated on ZEST underwent more cell divisions than their counterparts plated with no stroma, indicated by the reduction in PKH-26 fluorescence (Fig. 3C). Although few cells plated with no stroma progressed past one (lymphoid fraction) or two (precursor fraction) divisions, cells plated on ZEST underwent more than five divisions in the lymphoid and precursor fractions over 5 days. These data can be quantitated into a "division index," which is the average number of cell divisions that a cell in the original population underwent over the

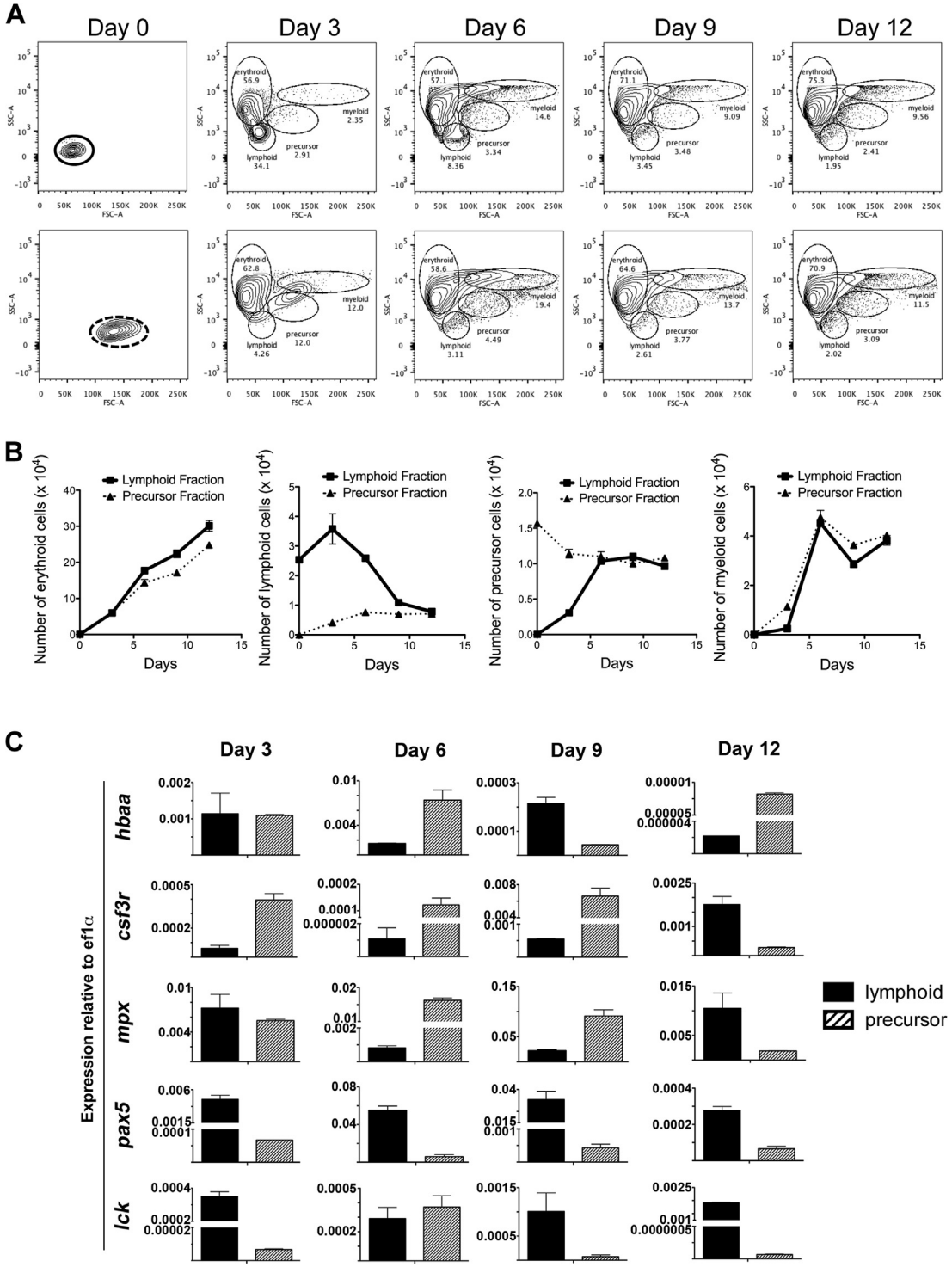

Figure 4. ZEST cells encourage differentiation of lymphoid and precursor cell fractions. **(A)** Isolated lymphoid (top left plot, *black line*) and precursor (bottom left plot, *dashed line*) cell fractions were plated on ZEST at day 0, and differentiated over the course of 12 days. Each day, cells were removed and investigated on a flow cytometer to determine changes in the cells' scatter profiles. **(B)** Isolated lymphoid (*squares, solid line*) and precursor (*triangles, dashed line*) cell fractions were plated on ZEST at day 0, and the number of differentiated erythroid (leftmost), lymphoid (second panel), precursor (third panel), and myeloid (rightmost) were enumerated over the course of 12 days. Flow cytometry plots in **(A)** were coupled with total cell counts at each time point to obtain these data. Each point represents the average of two biological replicates, and error bars represent SD. **(C)** Quantitative RT-PCR results from cells isolated from differentiated isolated lymphoid (*black bar*) and precursor (*striped bar*) cell fractions. At each time point, cells were interrogated for the erythroid-specific marker *hbaa* (top), myeloid markers *csf3r* and *mpx* (second and third rows), B-cell marker *pax5* (fourth row), and T-cell marker *lck* (bottom row). Bars represent the relative expression of two replicates averaged together, and error bars represent SD. Relative expression was determined by the $\Delta\Delta Ct$ method, using ef1α as a reference gene.

course of 5 days. Again, the division index of all cells plated on ZEST cells is at least two times higher than when no stroma is present. Together, these data indicate that ZEST cells facilitate HSPC proliferation.

ZEST cells support HSPC differentiation

To determine if ZEST cells also encouraged the differentiation of hematopoietic cells, we purified *ubi*:GFP$^+$ lymphoid and precursor populations by FACS and co-cultured them for 12 days on ZEST monolayers, adding iron supplement and carp serum to improve erythroid differentiation [30] (Fig. 4). In addition to identifying lymphoid and precursor fractions of zebrafish WKM by flow cytometry, it is also possible to identify mature myeloid and erythroid cells in this manner [40]. Purified lymphoid and precursor populations started to differentiate by day 3 in culture when analyzed by flow cytometry (Fig. 4A, top). The change in granularity of the lymphoid cells into erythroid, precursor, and myeloid fractions indicated that HSPCs present in this fraction had differentiated. Likewise, precursor cells changed their scatter characteristics to be more erythroid, lymphoid, and myeloid (Fig. 4A, bottom). This differentiation continued over the course of 12 days in culture. To quantitate the actual number of cells that were generated in these cultures, the percentages of *ubi*:GFP$^+$ WKM cells in particular cellular fractions (from Fig. 4A) were multiplied by the total number of WKM cells in the culture. Both lymphoid and precursor populations showed expansion of erythroid cells at every time point throughout the time course (Fig. 4B, leftmost panel). The precursor population had an increased number of lymphoid cells on days 3 and 6, eventually leveling out by day 9 and remaining relatively unchanged by day 12. On the other hand, the lymphoid population had an increased number of lymphoid cells at day 3, followed by a gradual decline that continued until day 12 (Fig. 4B, second panel), likely because the HSCs present in this population are rare; the majority of cells are postmitotic lymphocytes and do not proliferate over the course of 12 days. The plated lymphoid population showed an increase in precursor cells up to day 6, at which point they remained relatively constant for the remainder of the time course, whereas the plated precursor population exhibited a decrease in precursor cells over time, likely because these HSPCs were differentiating into mature hematopoietic lineages (Fig. 4B, third panel). Finally, both cells from lymphoid and precursor populations exhibited an expansion of mature myeloid cells over the course of the experiment (Fig. 4B, rightmost panel). To confirm that ZEST stroma encouraged the differentiation of HSPCs, RNA was extracted from these experiments and qRT-PCR was performed for mature hematopoietic markers. The erythroid-specific transcript *hbaa* was detected in both the lymphoid and precursor cultures at every time point during the assay, as were the myeloid-specific transcripts *mpx* and *csf3r* and the lymphoid-specific transcripts *pax5* and *lck* (Fig. 4C). Overall, the change in scatter profile, numbers, and gene expression indicate that HSPCs within the lymphoid and precursor fractions differentiated into mature myeloid, lymphoid, and erythroid cells when plated on ZEST cells.

Differentiation of clonal HSPCs on ZEST stroma

Because ZEST cells support multilineage differentiation of HSPCs, we hypothesized that they had utility to identify HSPCs in vitro. To develop an assay to test HSPC differentiation (Fig. 5A), we isolated cells from the WKM marked with the *cd41*:GFP transgene, previously identified as a marker for HSCs with in vivo experiments [45]. As previous work identified the lymphoid fraction as the scatter fraction in which HSCs were enriched [40], we isolated *cd41*:GFP$^+$ lymphoid cells from these fish and used FACS to deposit individual cells into individual wells of a 96-well plate. On this 96-well plate was a monolayer of ZEST cells with iron supplement and carp serum, and the *cd41*:GFP$^+$ cells were allowed to proliferate and differentiate over the course of 5 days. After 5 days, RNA was isolated from individual wells, cDNA was generated, and qRT-PCR was performed for lineage-specific markers, including the myeloid-specific transcripts *cmpl*, *cd41*, *csf1r*, *mpx*, and *mpeg*; the erythroid-specific *band3* and *hbaa*; the B cell-specific *igm* and *pax5*; and the T cell-specific *lck*. To simply the presentation of these data, we generated a color-coded schematic, whereby every column represents an individual well that received an individual *cd41*:GFP$^+$ cell that was interrogated for lineage-specific transcripts (Fig. 5). If there was any expression of that specific gene, a *colored box* is shown; a *black box* indicates no expression. All samples were normalized to *ef1α* as a housekeeping gene, so all columns have a *yellow box* in that row. All samples were also normalized to gene expression in the kidney, which is the far right column, also uniformly *yellow.* As a control, we performed qRT-PCR for the fold change in these markers when no *cd41*:GFP$^+$ cells were plated on ZEST cells; only very few wells indicated any levels of these markers (Fig. 5B). Importantly, no samples had multilineage transcript expression. However, when *cd41*:GFP$^+$ cells were plated on ZEST cells and allowed to differentiate for 5 days, there was a striking increase in numbers of wells that had multilineage transcript readouts. We considered a well (column) that had both myeloerythroid and lymphoid transcripts to be multilineage; 57% of wells had this characteristic (Fig. 5C). Importantly, only one of 49 samples failed to generate a hematopoietic readout, indicating that *cd41:GFP*$^+$ cells survive and differentiate well on the ZEST monolayer. Overall, these data indicate that ZEST cells are an excellent in vitro model for analyzing the differentiation capability of HSPCs. These assays should allow the identification and testing of putative HSPCs and the validation of previously identified HSPCs.

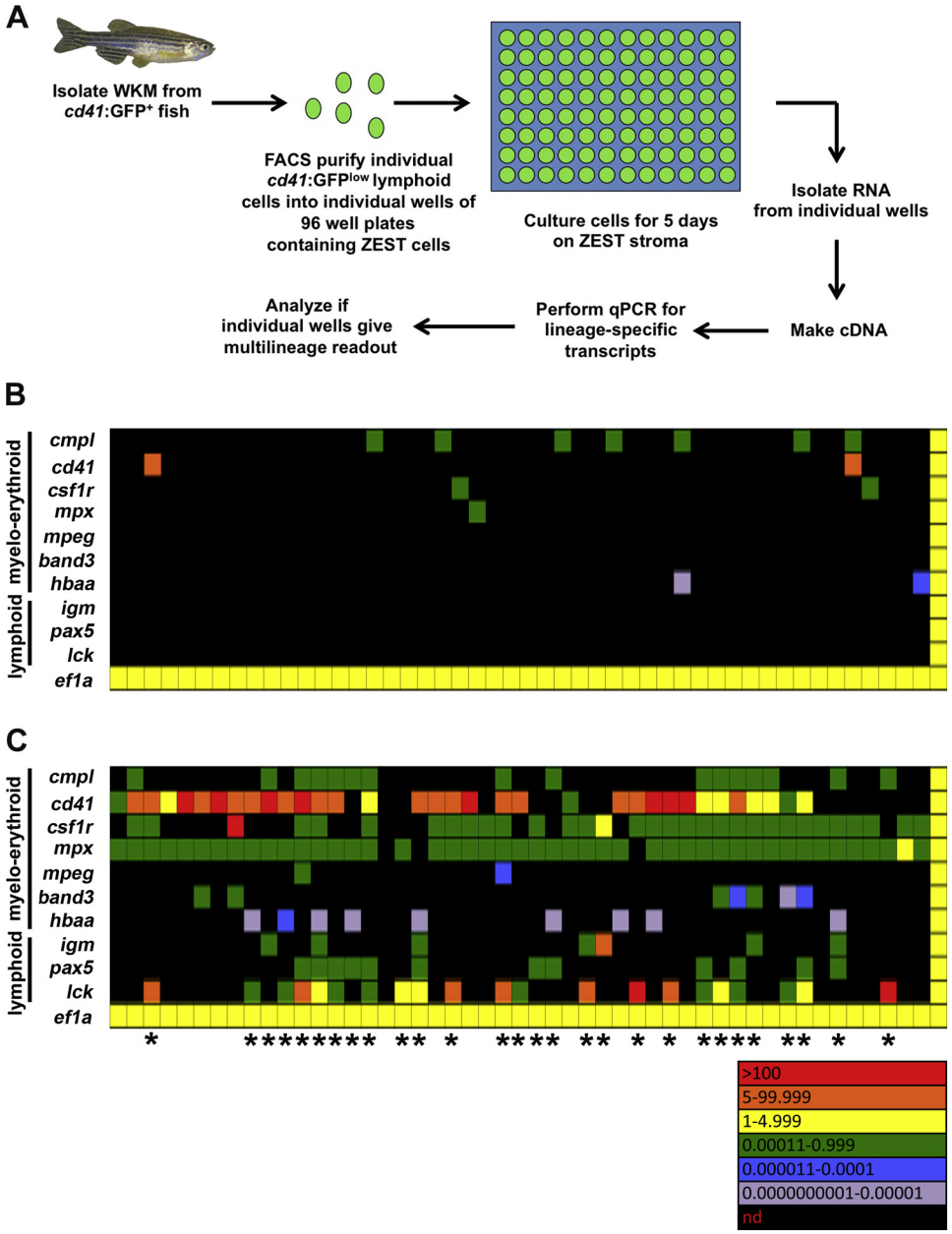

Figure 5. ZEST cells encourage multilineage differentiation of individual HSPCs. **(A)** Schematic of experiment. **(B)** Visualization of qRT-PCR results from ZEST cells only. Each column is an individual sample (ZEST stroma only) grown for 5 days in culture. Far right column is kidney. Samples were interrogated for the genes listed on left side of the figure. Different color boxes shown at the bottom of the figure represent fold expression relative to kidney. Fold expression was determined by the $\Delta\Delta Ct$ method, using ef1α as a reference gene and kidney as a reference tissue. **(C)** Visualization of qRT-PCR results from ZEST cells only. Each column is an individual sample (*cd41*:GFP^{low} cells plated on ZEST stroma) grown for 5 days in culture. Far right column is kidney. Samples were interrogated for the genes listed on left side of the figure. Different color boxes at the bottom of the figure represent fold expression relative to kidney. Fold expression was determined by the $\Delta\Delta Ct$ method, using ef1α as a reference gene and kidney as a reference tissue. If a column contained myeloerythroid markers and a lymphoid marker, it was scored as multilineage (demarcated with *).

ZEST and ZKS cells are different stromal cell lines

Although ZEST and ZKS cells both support HSPC proliferation and multilineage differentiation, they are derived from different temporal and spatial locations in the zebrafish. As such, we hypothesized that they would have different properties. First, we compared the ability of ZEST cells and ZKS cells to expand WKM in culture, plating cells and enumerating them over the course of 14 days. While ZKS expanded WKM, ZEST monolayers encouraged approximately four times more expansion over the course of the experiment (Fig. 6A), indicating that they had different expansion ability. To more thoroughly investigate the differences and similarities between these cell lines, we performed RNA sequencing (RNASeq) to analyze

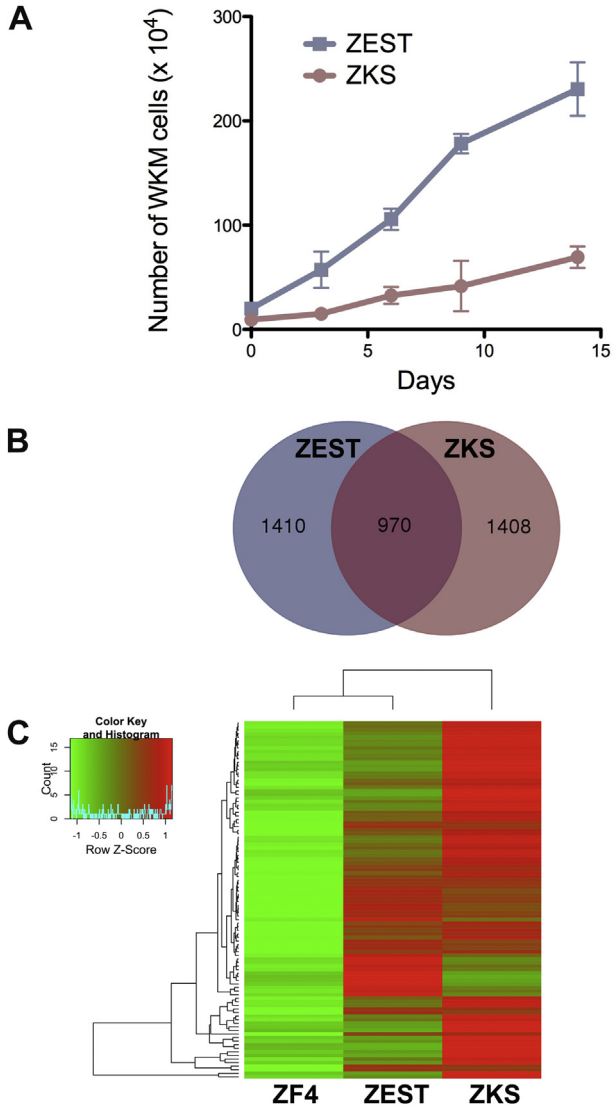

Figure 6. ZKS and ZEST cells both support hematopoiesis, but are different functionally and transcriptionally. **(A)** WKM cells plated on ZEST monolayers (*blue squares, solid line*) or ZKS monolayers (*red circles, solid line*) enumerated over 14 days. **(B)** Venn diagram indicating the number of transcripts at least twofold overexpressed in ZEST cells (*blue*, 2,380), ZKS cells (*red*; 2,378), and shared by both cell lines (intersection; 970) when compared with the non-hematopoietic-supportive ZF4 cell line. **(C)** Heat map representing the top 100 upregulated genes in ZEST or ZKS cells compared with ZF4 cells. *Green* represents underexpressed genes, and *red* denotes overexpression. Genes are listed in Table 2 in the same order (top-to-bottom), along with the RPKM values used to generate the heat map.

differences in the transcriptomes of ZEST and ZKS cells, comparing expressed transcripts in these cell lines to those of non-hematopoietic-supportive ZF4 stromal cells (data not shown). Although ZKS and ZEST cells shared 970 transcripts more than twofold upregulated when compared with ZF4 cells, our studies also indicated that ZEST cells expressed 1,410 unique transcripts from ZKS cells (Fig. 6B). Additionally, ZKS cells expressed 1,408 unique transcripts when compared with ZEST cells (Fig. 6B). To more carefully examine the expression differences between the shared upregulated transcripts, we took the top 100 genes overexpressed in both ZKS and ZEST cells (from the subset of 970 shared genes) and plotted their expression in a heat map (Fig. 6C and Table 2). In this figure, *green* represents genes expressed at levels similar to those of ZF4 cells, whereas red denotes genes more highly upregulated compared with ZF4 cells. These studies indicated that there are subsets of genes similarly overexpressed in ZKS and ZEST cells; analysis of gene ontology (GO) terms overrepresented in these 100 transcripts indicated that the top two enriched GO terms were "translation" and "protein metabolic processes," which fits with the fact that these stromal cells are producing hematopoietic-supportive proteins (Table 3). However, there are also subsets of genes expressed differentially in these cell types (Fig. 6C). The gene names of these top 100 genes are listed in Table 2 in the same order presented in Figure 6C, along with their reads per kilobase of transcript per million reads mapped (RPKM) values. Overall, these data indicate that although they appear to function similarly in support of hematopoiesis in vitro, ZEST and ZKS cells, have very different transcript expression.

Discussion

Over the past 20 years, zebrafish have become a more popular model system for investigating hematopoietic development and dysregulation. The transparency and external development of zebrafish have been instrumental in observing early hematopoietic ontogeny, and the ability to perform large-scale mutagenesis and drug screens has been critical in the identification of genes and pathways involved in hematopoiesis. However, the zebrafish as a model system has traditionally lacked the functional assays needed to investigate HSPC proliferation and differentiation. Importantly, HSPCs are essential to understanding molecular pathways essential for hematopoiesis; these multi-, oligo-, and unipotent cells are commonly dysregulated during hematologic disease [48–50].

Hematopoietic stem and progenitor cells in mammals were discovered and characterized largely because of the development of in vitro assays to functionally assess their differentiation capabilities [51–54]. As HSPCs were not well defined in zebrafish, yet are essential to understanding, preventing, and treating hematologic disorders, we designed assays to investigate them. Our first studies involved creating ZKS cells, a stromal cell line from adult zebrafish, which is the main site of hematopoiesis in teleosts. These cells allowed the rescue of erythroid genetic mutants, underlining their usefulness in investigating the differentiation of HSPCs [30]. ZKS cells also expressed multiple cytokines such as *epo*, *gcsfa*, *gcsfb*, and *tpo*, allowing the development of clonal methylcellulose assays to

Table 2. Top 100 transcripts overexpressed in hematopoietic-supportive ZKS and ZEST cells compared with non–hematopoietic-supportive ZF4 cells[a]

Gene	RPKM (ZKS)	RPKM (ZEST)	RPKM (ZF4)
mustn1a	191.7311182	94.20002244	2.377441447
myl9a	179.6584981	96.56364658	2.276630133
si:busm1-57f23.1	182.0504465	89.25803193	13.64267158
blmh	184.0111916	86.10283629	29.39759063
cmbl	196.7707245	73.67679014	26.91899859
scinla	229.2763242	77.71766924	1.171371221
pycard	216.1110211	70.80059954	0.244784777
wfdc2	215.3192844	100.2819887	5.805860073
atp6v1e1b	211.5850639	104.0432062	50.77535662
tnfaip6	197.4394341	109.3081398	52.44479497
arl6ip5b	180.1080903	105.0459892	49.94297373
ndufb11	247.4927535	68.49972903	30.78048579
psma6a	227.9565636	80.43925949	36.57643139
rpl13a	262.095085	85.45651864	42.49472207
si:dkey-100n23.4	241.0388676	112.7794318	26.3597982
rnd3b	230.919067	106.1477521	20.10791448
Ada	235.815493	146.7960562	31.49486791
rpz5	239.9595079	157.8233757	7.805466586
vmhc	277.2773505	124.2928784	3.342640338
cahz	355.7589188	56.55174506	1.48171963
ost4	293.697141	56.14183101	22.3880387
txn	428.0840844	170.734287	74.95409787
fhl1a	392.740221	209.8129055	51.64958797
si:dkey-12l12.1	431.6353641	159.7228348	29.13243458
ckba	410.942751	156.7429014	16.93871335
phex	374.7902084	246.0473474	1.422658424
CABZ01024686.1	320.0454925	195.9867392	0.150924627
rsl24d1	303.7118765	226.5305973	110.1637925
ap2m1a	256.7847085	248.5305894	108.62445
dlx3b	285.6044597	300.5094173	33.95661813
adamtsl7	377.7311012	296.1991765	75.65003739
anxa1a	386.1286169	280.2930981	71.0710686
cdk1	157.1526365	92.45941086	41.08086644
ENSDARG00000087773 (novel gene, no gene name)	151.3186816	86.06460141	36.7259713
lgals3l	151.485882	94.79980323	28.5517658
mcl1b	138.0029954	100.3628761	34.55007944
sumo3b	142.0062334	85.88205698	40.71745045
cx4oi2	157.1675799	83.44086012	13.50501713
capgb	140.0313977	95.47507416	14.03742087
fibina	162.385075	111.5193532	8.63161174
dcn	138.738941	110.0299673	2.200388725
fpr1	129.1084434	117.6367545	0.801762529
hspb9	208.1065389	130.9142075	4.453978651
urah	181.7492844	153.0214309	2.606067373
id3	123.0298414	119.957024	32.53271352
cd82 b	117.1867309	119.7501676	20.88039052
dkk1b	115.2674028	123.3601222	3.914853583
cx43	95.76255571	125.268914	20.60977394
phlda3	103.4830928	114.8205638	42.38678055
pitpnaa	102.4114719	110.3454892	46.22327706
tstd1	91.48324211	99.41705808	27.77823182
timp2a	110.5132145	134.7435353	45.08674135
igflr1	107.6665533	126.7691791	49.45986261
ctsh	116.9107597	129.9969604	52.32102958
tspan4b	124.4627775	134.439824	38.31343901
kctd12.2	70.17791498	131.2071169	10.41369721
anxa5b	223.4276827	190.0509067	82.02660608
ccnd1	204.0826607	198.000819	77.64559053
cnn3a	200.6466151	175.5868376	85.12488537
lmo4b	171.4754089	158.0390988	54.76838861
iscu	177.5601397	135.6039718	62.57678042
serpine2	155.1438879	185.8865435	41.16096343
cxcl-c1c	205.5342189	222.3706168	33.03549542
fabp7a	195.9918097	237.0929702	21.40297666
si:ch211-174h4.1	224.7857597	199.3655569	38.63959992
ehd2	161.7766861	245.0843826	56.47716098
crabp2b	105.0984741	221.8625863	49.8034191
si:ch211-222d3.3	95.00787666	229.3358097	21.15952131
dusp5	126.478358	236.8883821	9.107537686
itga10	89.61611629	201.1502394	2.352461298
tcn2l	38.72650992	164.8295692	13.11416496
cyp24a1	18.72705544	177.0835255	2.519571099
gdf10 b	33.67260166	219.1972506	0.695893287
hpdb	81.65105717	369.7602972	1.681026612
hbegfa	237.5287195	432.953554	115.5311657
timp2b	201.697207	353.6519834	68.67404428
thbs4b	211.3951489	552.8064964	31.77418366
phlda2	661.6069058	447.6778629	148.3523463
prdx1	663.2337466	378.8825097	122.1185737
gstp1	585.6433683	324.3995674	107.5635844
sncga	506.5409161	491.6240584	33.91588988
calm3a	398.2576181	445.6855878	77.36093147
ENSDARG00000092903 (novel gene, gene name projected to be *C18H15orf48*)	570.4850827	238.5350614	41.45849625
cd9b	506.2882968	266.2312285	25.2919086
snrpe	514.8853227	160.8159508	78.98388808
rpl31	786.6591853	197.9255876	69.5006252
ifitm5	617.8582984	44.28435681	0.866051404
soul5	827.0453265	703.7188802	13.01478191
rps16	1058.353433	295.6625046	126.4458616
rpl10a	935.7242298	364.8865983	139.5790661
si:dkey-22i16.3	966.7386902	8.207114594	1.997906106
ENSDARG00000071626 (novel gene; no gene name)	858.6043295	26.27619774	1.428567107
rps9	1642.964348	524.3909043	228.2500494
cox6b1	1642.244168	266.1138185	132.3260874
si:ch211-12e1.3	1538.960816	697.6199432	27.15657434
rpl22	1350.323073	497.4139112	219.2842156
clu	1178.602248	1219.222027	348.8825399
stc2a	1171.390702	1231.42446	164.7996506
rpl32	3503.451624	1012.274554	501.3860264
rpl6	3084.841751	1276.133337	501.4586706

[a]Gene names listed based on Zv9 assembly, as well as reads per kilobase of transcript per million reads mapped (RPKM) of ZKS, ZEST, and ZF4 samples.

further refine the isolation and testing of zebrafish HSPCs [31,36,44]. Although methylcellulose assays allowed the clonal investigation of myeloerythroid HSPCs, assays to assess lymphoid progenitors remain elusive; lympho-supportive cytokines have yet to be identified and

Table 3. GO terms enriched in top 100 transcripts overexpressed in hematopoietic-supportive ZKS and ZEST cells compared with non-hematopoietic-supportive ZF4 cells[a]

Term	Description	Count	%	*p* Value	Gene	List total	Pop hits	Pop total	Fold enrichment	Bonferroni	Benjamini	FDR
GO:0006412	Translation	9	10.46511628	1.76E-04	*rps16, rpl22, rpl10a, rsl24d1, rpl32, rps9, rpl6, rpl13a, rpl31*	53	260	8,389	5.479027576	0.06396177	0.06396177	0.24324761
GO:0016265	Death	4	4.651162791	0.010687242	*phlda3, ckba, clu, pycard*	53	74	8,389	8.555838858	0.98221296	0.866631938	13.79658808
GO:0008219	Cell death	4	4.651162791	0.010687242	*phlda3, ckba, clu, pycard*	53	74	8,389	8.555838858	0.98221296	0.866631938	13.79658808
GO:0007423	Sensory organ development	5	5.813953488	0.040593182	*ccnd1, dkk1b, scinla, atp6v1e1b, dlx3b*	53	210	8,389	3.768643306	0.999999822	0.994372052	43.5930556
GO:0019538	Protein metabolic process	17	19.76744186	0.052330213	*dusp5, ctsh, rps16, rpl6, rpl13a, pycard, serpine2, psma6a, sumo3b, rpl22, blmh, rpl10a, rsl24d1, rpl32, rps9, phex, rpl31*	53	1719	8,389	1.565335265	0.999999998	0.993519671	52.41499751
GO:0001654	Eye development	4	4.651162791	0.060506013	*ccnd1, scinla, atp6v1e1b, dlx3b*	53	145	8,389	4.366428107	1	0.990730627	57.78407743
GO:0012501	Programmed cell death	3	3.488372093	0.071435474	*phlda3, ckba, pycard*	53	71	8,389	6.688014882	1	0.990266803	64.08636132
GO:0006915	Apoptosis	3	3.488372093	0.071435474	*phlda3, ckba, pycard*	53	71	8,389	6.688014882	1	0.990266803	64.08636132
GO:0042770	DNA damage response, signal transduction	2	2.325581395	0.077705368	*ccnd1, phlda3*	53	13	8,389	24.35123367	1	0.986877438	67.29575354
GO:0009888	Tissue development	5	5.813953488	0.096534022	*dkk1b, cx43, dcn, vmhc, dlx3b*	53	282	8,389	2.806436505	1	0.991422401	75.40577817

[a]GO terms and description of transcripts in Table 2 analyzed by Database for Annotation, Visualization and Integrated Discovery (DAVID) v6.7 [46,47]. Gene names listed based on Zv9 assembly.

recombinantly generated, and T-cell development requires cell-to-cell contact [55]. The benefit of ZKS and ZEST cells is that they do support lymphoid cell proliferation and differentiation, likely by their expression of lympho-supportive cytokines and Notch ligands. Further examination of the transcriptomes of these 2 cell lines is likely to yield important advances in this area.

Importantly, stromal cells are useful for understanding not only normal hematopoiesis, but also the effect of the hematopoietic niche on hematologic disease development [56]. Other groups created zebrafish hematopoietic-supportive mesenchymal stem cell lines from *sdf1*:DsRed transgenic animals [57], allowing investigation of the hematopoietic niche, positing the zebrafish as a useful model system to study niche/HSPC interactions. Importantly, ZEST cells are easily transfected, and with the advent of CRISPR/Cas9 technology, it should be possible to quickly and effectively modulate putatively important stromal factors involved in hematopoiesis in this in vitro system.

Zebrafish embryonic stromal trunk cells, like their ZKS counterparts, appear to resist senescence. ZEST cells have been grown for more than 100 passages, never underwent a massive die off followed by a clonal recovery during their establishment, and show no growth slowing or functional deviation. We have created 10 different clonal lines of ZEST cells, and all have the same functional properties; they all support the expansion and differentiation of hematopoietic cells (data not shown). Also, similar to ZKS cells, ZEST cells support the proliferation and differentiation of all blood cells; lymphoid cells and myeloid cell types were expanded and observed. Although ZEST cells do not support the survival of postmitotic red blood cells for more than 6 days in culture, they do encourage differentiation from erythroid precursors when iron supplement and carp serum are added to isolated HSPCs. While ZEST cells support adult HSPCs, future experiments are required to analyze embryonic HSPCs. However, as ZKS cells support embryonic HSPCs [58], we believe ZEST cells also will. Because of their embryonic origin, they may be more supportive.

The gold standard for identifying HSCs is the transplantation of putative HSCs into irradiated recipients and measurement of long-term hematopoietic reconstitution. In mice, studies indicate that only 0.01% of bone marrow (the mammalian location of HSCs, equivalent to fish WKM) is composed of long- and short-term HSCs [59]. In zebrafish, these studies have been problematic; few clonal fish strains exist, so immune-matching donors and recipients is challenging. Because of these issues, it has been difficult to quantitate zebrafish HSCs. Descriptive reports quantitating side-population (SP) HSCs indicated that $0.056 \pm 0.008\%$ of the WKM is composed of SP HSCs [60], but this characterization was largely descriptive; there was no functional evidence that these cells were bona fide HSCs. Further refinement of this SP assay indicated that

20% of these SP cells in *cd41*:GFP transgenic animals expressed *cd41* at low levels [45]. Transplanting these *cd41*:GFP^{low} SP cells rescued irradiated hosts, indicating that about 0.018% of the WKM is composed of HSCs [45]. However, these studies did not isolate *cd41*:GFP^{low} cells from the lymphoid scatter fraction, the fraction where HSCs reside [40]. Additionally, these studies did not immune-match donors and recipients, likely reducing the amount of successful engraftment and long-term reconstitution.

We took a different approach to quantitating zebrafish progenitors, developing a clonal in vitro assay to assess if they had the capability of multilineage differentiation. By plating *cd41*:GFP^{low} cells from the lymphoid scatter fraction on ZEST cells and analyzing a multilineage transcriptional readout 5 days later, we were able to enumerate HSPCs present in the zebrafish kidney. Our FACS isolation indicated that *cd41*:GFP^{low} cells in the lymphoid fraction routinely constituted 0.3% of the total WKM. We detected both lymphoid and myeloerythroid differentiation from 57% of these cells, or 0.171% of the WKM. This percentage is higher than the estimated numbers of *cd41*:GFP^{low} HSCs present in this population [45], indicating that this population is heterogeneous [45] and that our assay detects other multipotent progenitors in this population. Further refinement of the assay, including sorting SP^{+} *cd41*:GFP^{low} lymphoid cells, may resolve this issue. Although we cannot assess if these *cd41*:GFP^{low} lymphoid cells are bona fide HSCs with this assay, they represent a progenitor pool that expressed multiple mature hematopoietic lineage transcripts after culture on ZEST cells.

Acknowledgments

This research was supported by National Institutes of Health Grants K01-DK087814-01A1 (DLS) and R01 DK074482 (DT).

Author contributions

DLS and DT designed the research. CC, TS, RPL, AS, PCL, BA, JA, EH, and DLS performed research. DLS and DT wrote the article.

Conflict of interest disclosure

All authors declare no competing financial interests.

References

1. Orkin SH, Zon LI. Hematopoiesis: an evolving paradigm for stem cell biology. Cell. 2008;132:631–644.
2. Carroll KJ, North TE. Oceans of opportunity: exploring vertebrate hematopoiesis in zebrafish. Exp Hematol. 2014;42:684–696.
3. Carradice D, Lieschke GJ. Zebrafish in hematology: sushi or science? Blood. 2008;111:3331–3342.
4. Boatman S, Barrett F, Satishchandran S, Jing L, Shestopalov I, Zon LI. Assaying hematopoiesis using zebrafish. Blood Cells Mol Dis. 2013;51:271–276.
5. Bertrand JY, Chi NC, Santoso B, Teng S, Stainier DY, Traver D. Haematopoietic stem cells derive directly from aortic endothelium during development. Nature. 2010;464:108–111.
6. Kissa K, Herbomel P. Blood stem cells emerge from aortic endothelium by a novel type of cell transition. Nature. 2010;464:112–115.
7. Mathias JR, Dodd ME, Walters KB, Yoo SK, Ranheim EA, Huttenlocher A. Characterization of zebrafish larval inflammatory macrophages. Dev Comp Immunol. 2009;33:1212–1217.
8. Renshaw SA, Loynes CA, Trushell DM, Elworthy S, Ingham PW, Whyte MK. A transgenic zebrafish model of neutrophilic inflammation. Blood. 2006;108:3976–3978.
9. Ellett F, Pase L, Hayman JW, Andrianopoulos A, Lieschke GJ. mpeg1 promoter transgenes direct macrophage-lineage expression in zebrafish. Blood. 2011;117:e49–56.
10. Hall C, Flores MV, Storm T, Crosier K, Crosier P. The zebrafish lysozyme C promoter drives myeloid-specific expression in transgenic fish. BMC Dev Biol. 2007;7:42.
11. Herbomel P, Thisse B, Thisse C. Ontogeny and behaviour of early macrophages in the zebrafish embryo. Development. 1999;126:3735–3745.
12. Lieschke GJ, Oates AC, Crowhurst MO, Ward AC, Layton JE. Morphologic and functional characterization of granulocytes and macrophages in embryonic and adult zebrafish. Blood. 2001;98:3087–3096.
13. Bennett CM, Kanki JP, Rhodes J, et al. Myelopoiesis in the zebrafish, *Danio rerio*. Blood. 2001;98:643–651.
14. Lugo-Villarino G, Balla KM, Stachura DL, Banuelos K, Werneck MB, Traver D. Identification of dendritic antigen-presenting cells in the zebrafish. Proc Natl Acad Sci USA. 2010;107:15850–15855.
15. Willett CE, Zapata AG, Hopkins N, Steiner LA. Expression of zebrafish rag genes during early development identifies the thymus. Dev Biol. 1997;182:331–341.
16. Driever W, Solnica-Krezel L, Schier AF, et al. A genetic screen for mutations affecting embryogenesis in zebrafish. Development. 1996;123:37–46.
17. Weinstein BM, Schier AF, Abdelilah S, et al. Hematopoietic mutations in the zebrafish. Development. 1996;123:303–309.
18. Ransom DG, Haffter P, Odenthal J, et al. Characterization of zebrafish mutants with defects in embryonic hematopoiesis. Development. 1996;123:311–319.
19. Ridges S, Heaton WL, Joshi D, et al. Zebrafish screen identifies novel compound with selective toxicity against leukemia. Blood. 2012;119:5621–5631.
20. Yeh JR, Munson KM, Elagib KE, Goldfarb AN, Sweetser DA, Peterson RT. Discovering chemical modifiers of oncogene-regulated hematopoietic differentiation. Nat Chem Biol. 2009;5:236–243.
21. Clements WK, Traver D. Fish pharming: zebrafish antileukemia screening. Blood. 2012;119:5614–5615.
22. Bowman TV, Zon LI. Swimming into the future of drug discovery: in vivo chemical screens in zebrafish. ACS Chem Biol. 2010;5:159–161.
23. Peterson RT, Shaw SY, Peterson TA, et al. Chemical suppression of a genetic mutation in a zebrafish model of aortic coarctation. Nat Biotechnol. 2004;22:595–599.
24. Brownlie A, Hersey C, Oates AC, et al. Characterization of embryonic globin genes of the zebrafish. Dev Biol. 2003;255:48–61.
25. North TE, Goessling W, Walkley CR, et al. Prostaglandin E2 regulates vertebrate haematopoietic stem cell homeostasis. Nature. 2007;447:1007–1011.
26. Mizgirev I, Revskoy S. Generation of clonal zebrafish lines and transplantable hepatic tumors. Nature protocols. 2010;5:383–394.
27. Mizgirev IV, Revskoy S. A new zebrafish model for experimental leukemia therapy. Cancer Biol Ther. 2010;9:895–902.

28. Smith AC, Raimondi AR, Salthouse CD, et al. High-throughput cell transplantation establishes that tumor-initiating cells are abundant in zebrafish T-cell acute lymphoblastic leukemia. Blood. 2010;115: 3296–3303.
29. de Jong JL, Burns CE, Chen AT, et al. Characterization of immune-matched hematopoietic transplantation in zebrafish. Blood. 2011; 117:4234–4242.
30. Stachura DL, Reyes JR, Bartunek P, Paw BH, Zon LI, Traver D. Zebrafish kidney stromal cell lines support multilineage hematopoiesis. Blood. 2009;114:279–289.
31. Stachura DL, Svoboda O, Lau RP, et al. Clonal analysis of hematopoietic progenitor cells in the zebrafish. Blood. 2011;118:1274–1282.
32. Liongue C, Ward AC. Evolution of Class I cytokine receptors. BMC Evol Biol. 2007;7:120.
33. Lin HF, Traver D, Zhu H, et al. Analysis of thrombocyte development in CD41-GFP transgenic zebrafish. Blood. 2005;106:3803–3810.
34. Mosimann C, Kaufman CK, Li P, Pugach EK, Tamplin OJ, Zon LI. Ubiquitous transgene expression and Cre-based recombination driven by the ubiquitin promoter in zebrafish. Development. 2011;138:169–177.
35. Stachura DL, Traver D. Cellular dissection of zebrafish hematopoiesis. Methods in cell biology. 2011;101:75–110.
36. Stachura DL, Svoboda O, Campbell CA, et al. The zebrafish granulocyte colony-stimulating factors (Gcsfs): 2 paralogous cytokines and their roles in hematopoietic development and maintenance. Blood. 2013;122:3918–3928.
37. Bertrand MJ, Kenchappa RS, Andrieu D, et al. NRAGE, a p75NTR adaptor protein, is required for developmental apoptosis in vivo. Cell Death Differ. 2008;15:1921–1929.
38. Bertrand JY, Kim AD, Teng S, Traver D. CD41+ cmyb+ precursors colonize the zebrafish pronephros by a novel migration route to initiate adult hematopoiesis. Development. 2008;135:1853–1862.
39. Wittamer V, Bertrand JY, Gutschow PW, Traver D. Characterization of the mononuclear phagocyte system in zebrafish. Blood. 2011;117: 7126–7135.
40. Traver D, Paw BH, Poss KD, Penberthy WT, Lin S, Zon LI. Transplantation and in vivo imaging of multilineage engraftment in zebrafish bloodless mutants. Nat Immunol. 2003;4:1238–1246.
41. Langmead B, Salzberg SL. Fast gapped-read alignment with Bowtie 2. Nat Methods. 2012;9:357–359.
42. Paffett-Lugassy N, Hsia N, Fraenkel PG, et al. Functional conservation of erythropoietin signaling in zebrafish. Blood. 2007;110:2718–2726.
43. Liongue C, Hall CJ, O'Connell BA, Crosier P, Ward AC. Zebrafish granulocyte colony-stimulating factor receptor signaling promotes myelopoiesis and myeloid cell migration. Blood. 2009;113:2535–2546.
44. Svoboda O, Stachura DL, Machonova O, et al. Dissection of vertebrate hematopoiesis using zebrafish thrombopoietin. Blood. 2014; 124:220–228.
45. Ma D, Zhang J, Lin HF, Italiano J, Handin RI. The identification and characterization of zebrafish hematopoietic stem cells. Blood. 2011; 118:289–297.
46. Huang da W, Sherman BT, Zheng X, et al. Extracting biological meaning from large gene lists with DAVID. Curr Protoc Bioinformatics. 2009; Chapter 13:Unit 13.11.
47. Huang da W, Sherman BT, Lempicki RA. Systematic and integrative analysis of large gene lists using DAVID bioinformatics resources. Nat Protoc. 2009;4:44–57.
48. Xu L, Gu ZH, Li Y, et al. Genomic landscape of CD34+ hematopoietic cells in myelodysplastic syndrome and gene mutation profiles as prognostic markers. Proc Natl Acad Sci USA. 2014;111: 8589–8594.
49. Brown BD. A shot in the bone corrects a genetic disease. Mol Ther. 2015;23:614–615.
50. Xie M, Lu C, Wang J, et al. Age-related mutations associated with clonal hematopoietic expansion and malignancies. Nat Med. 2014; 20:1472–1478.
51. Kondo M, Weissman IL, Akashi K. Identification of clonogenic common lymphoid progenitors in mouse bone marrow. Cell. 1997;91: 661–672.
52. Akashi K, Traver D, Miyamoto T, Weissman IL. A clonogenic common myeloid progenitor that gives rise to all myeloid lineages. Nature. 2000;404:193–197.
53. Nakorn TN, Miyamoto T, Weissman IL. Characterization of mouse clonogenic megakaryocyte progenitors. Proc Natl Acad Sci USA. 2003;100:205–210.
54. Mori Y, Iwasaki H, Kohno K, et al. Identification of the human eosinophil lineage-committed progenitor: revision of phenotypic definition of the human common myeloid progenitor. J Exp Med. 2009;206: 183–193.
55. Schmitt TM, Zuniga-Pflucker JC. Induction of T cell development from hematopoietic progenitor cells by delta-like-1 in vitro. Immunity. 2002;17:749–756.
56. Bulycheva E, Rauner M, Medyouf H, et al. Myelodysplasia is in the niche: novel concepts and emerging therapies. Leukemia. 2015;29: 259–268.
57. Lund TC, Patrinostro X, Kramer AC, et al. sdf1 Expression reveals a source of perivascular-derived mesenchymal stem cells in zebrafish. Stem Cells. 2014;32:2767–2779.
58. Bertrand JY, Kim AD, Violette EP, Stachura DL, Cisson JL, Traver D. Definitive hematopoiesis initiates through a committed erythromyeloid progenitor in the zebrafish embryo. Development. 2007; 134:4147–4156.
59. Domen JWA, Weissman I. Bone Marrow (Hematopoietic) Stem Cells. Vol. 2011. Bethesda, MD: National Institutes of Health, US Department of Health and Human Services: Stem Cell Information; 2011.
60. Kobayashi I, Saito K, Moritomo T, Araki K, Takizawa F, Nakanishi T. Characterization and localization of side population (SP) cells in zebrafish kidney hematopoietic tissue. Blood. 2008;111: 1131–1137.